



HAL
open science

Return of the Atacama deep Slow Slip Event: The 5-year recurrence confirmed by continuous GPS

Emilie Klein, Christophe Vigny, Zacharie Duputel, Dimitri Zigone, Luis Rivera, Sergio Ruiz, Bertrand Potin

► **To cite this version:**

Emilie Klein, Christophe Vigny, Zacharie Duputel, Dimitri Zigone, Luis Rivera, et al.. Return of the Atacama deep Slow Slip Event: The 5-year recurrence confirmed by continuous GPS. *Physics of the Earth and Planetary Interiors*, 2023, 334, pp.106970. 10.1016/j.pepi.2022.106970 . hal-04247779

HAL Id: hal-04247779

<https://hal.science/hal-04247779v1>

Submitted on 18 Oct 2023

HAL is a multi-disciplinary open access archive for the deposit and dissemination of scientific research documents, whether they are published or not. The documents may come from teaching and research institutions in France or abroad, or from public or private research centers.

L'archive ouverte pluridisciplinaire **HAL**, est destinée au dépôt et à la diffusion de documents scientifiques de niveau recherche, publiés ou non, émanant des établissements d'enseignement et de recherche français ou étrangers, des laboratoires publics ou privés.

Copyright

Return of the Atacama deep Slow Slip Event : the 5-year recurrence confirmed by continuous GPS

E. Klein¹, C. Vigny¹, Z. Duputel², D. Zigone³, L. Rivera³, S. Ruiz⁴, B. Potin⁴

¹Laboratoire de géologie, Département de Géosciences, ENS, CNRS, UMR 8538, PSL research University, Paris, France

²Observatoire Volcanologique du Piton de la Fournaise, Université de Paris, Institut de Physique du Globe de Paris, CNRS, F-75005, Paris, France

³Institut Terre & Environnement Strasbourg (ITES), UMR7063, Université de Strasbourg/CNRS ; Strasbourg, France

⁴Departamento de Geofísica, Universidad de Chile, Santiago, Chile

This is a postprint that has been peer-reviewed and is accepted for publication in *Physics of the Earth and Planetary Interiors* : <https://doi.org/10.1016/j.pepi.2022.106970>.

Abstract

Four years ago, using survey GPS measurements, the first deep slow slip event (SSE) was detected in Chile (near Copiapó, Atacama region), unrelated to any major earthquake. It was located between 40 and 60 km depth on the subduction interface, lasted approximately 18 months (2014-2016.5) and reached an equivalent magnitude of Mw 6.9. The single permanent station operating in the region between 2002 and 2015 revealed that similar events had occurred at least twice before around 2006 and 2010, suggesting a 5-year repeat time. In anticipation of the next event expected for 2020, we densified the existing continuous GNSS network in the region with 5 new stations in early 2019. Here we show that the SSE occurred in 2020 as expected with the 5 year recurrence time. The event started around March 2020 and developed during 6 months, before it was perturbed by the 2020 Atacama seismic sequence that occurred nearby. During those initial 6 months, the 2020 event had the same characteristics as the 2014 SSE. It occurred in the same area and at the same depth, repeating similar a pattern of surface deformation. Before the occurrence of the nearby seismic sequence of September 2020, it had reached a third of the total amplitude of the 2014 SSE which had lasted three times longer. Whether the 2020 SSE was aborted when the nearby seismic sequence occurred or continued in the background is unknown but this will be resolved with longer times series.

Corresponding author: E., Klein , klein@geologie.ens.fr

South America

Subduction zone processes

Seismic cycle

Transient deformation

Earthquake interaction, forecasting, and prediction

Space geodetic surveys

Key Points:

- The 5-year recurrence of the Atacama deep SSE is confirmed
- The first third of the 2014 and 2020 SSEs are very similar

1 Introduction

Over the last decades, many Slow-Slip Events (SSEs) have been detected and quantified along various subduction zones [e.g. *Beroza and Ide, 2011; Peng and Gomberg, 2010; Schwartz and Rokosky, 2007*]. Sizes, depths and durations are highly variable [e.g. *Wallace and Beavan, 2010*]. Some SSEs occur periodically [e.g. *Rogers and Dragert, 2003; Radiguet et al., 2012*]. So far, and despite being one of the most active regions in the world, only two slow slip events have been observed in Chile on the shallow part of the interface. Both lasted only several days to a few weeks, were associated with some seismic activity and followed by a significant earthquake: The Iquique sequence of 2014 [*Ruiz et al., 2014; Boudin et al., 2022*] and the Valparaiso sequence of 2017 [*Ruiz et al., 2017; Caballero et al., 2021*]. A longer SSE was detected preceding the Iquique earthquake, but with a very small amplitude [deviation of 2mm/yr in 8 months *Socquet et al., 2017*]. In the same time, only one truly silent SSE has been observed and documented on the Chilean megathrust. It occurred between 2014 and 2016 in the Atacama region of Chile ($\sim 27.5^\circ\text{S}$), where the Copiapó Ridge is subducted and offshore persistent seismic swarms have been detected in 1973, 1979 and 2006 [e.g. *Holtkamp et al., 2011*]. (Fig. 1-A). The 2014-2016 SSE was particularly deep (between 40 km and 60 km) and long lasting (at least 1.5 year s) [*Klein et al., 2018a*]. It also seemed plausible, although supported only by the records of the single continuous GPS (cGPS) station operating in the region at the time, that at least two other similar events had occurred in the same area in 2005 and 2009, suggesting a ~ 5 -year recurrence time. Finally, non volcanic tremors and clusters of similar events have recently been detected nearby [*Pastén-Araya et al., 2022*]. Altogether this depicts an interesting area with characteristics seemingly similar to what has been observed in other, better-instrumented regions (e.g. Cascadia, South-West Japan and Alaska), where long-term periodic SSEs are observed [*Rogers and Dragert, 2003; Obara and Kato, 2016; Rousset, 2019*]. The hypothesis of a 5-year recurrence motivated an effort initiated in 2019 to densify the instrumentation in the region (Fig. 1-A). Here, we investigate the characteristics of a transient event that did occur there in 2020, to confirm whether we are in the presence of the expected recurrent SSE.

2 GPS observations

2.1 Data processing

After the detection of the 2014-2015 slow slip event, in early 2019, we installed 5 continuous GPS (cGPS) stations in the Atacama region in order to densify the CSN network [*Báez et al., 2018*]. Overall, we now benefit from 12 cGPS stations located in the region of

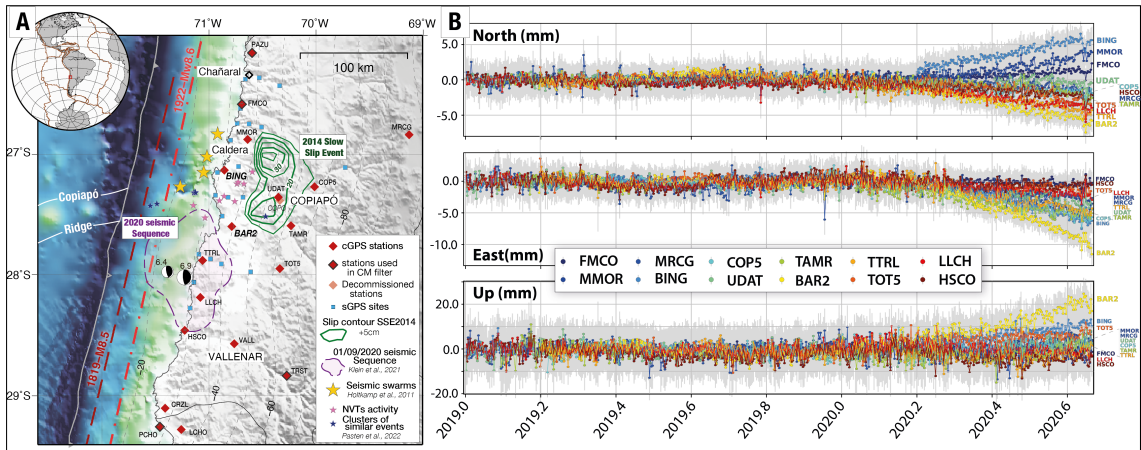


Figure 1. A. Seismo-tectonic context of the region. 2014 Slow slip Event distribution (green isolines are represented every 5 cm) from [Klein *et al.*, 2018b]. Survey (blue squares) and continuous GPS (red diamonds) networks of the region. Slab isodepths from Slab1.0 [Hayes *et al.*, 2012]. Yellow stars offshore Caldera depict seismic swarms that occurred in [1973, 1976, 2006, Holtkamp *et al.*, 2011, and 2015]. Blue stars depict clusters of similar events and pink stars NVTs activity [Pastén-Araya *et al.*, 2022]. The region of the 2020 sequence [including the relocated catalog of the seismic sequence and geodetic slip distributions of the 2 largest events and of the first month of post-seismic, Klein *et al.*, 2021] is depicted by the violet dashed area. B. Detrended and filtered time series of cGPS stations of the region.

interest (Fig. 1-A). For this study, we use the time series database *SOAM_GNSS_solENS* [Klein *et al.*, 2022], processed in double difference using the GAMIT/GLOBK software and aligned with the ITRF2014 using the PYACS toolbox [Herring *et al.*, 2018; Nocquet and Tran].

The time window runs for ~ 20 months, from 2019.0, the date at which the full network becomes operational, to 2020.7 (or 31/08/2020), the date at which the 2020 Atacama seismic crisis of nearby Totoral blurs the signal [Klein *et al.*, 2021]. Over this period of time, we first estimate and remove an overall trend from all time series, in order to be able to quantify and remove any instrumental offset. Then we filter the time series using a common mode filter built with four stations surrounding the region (FMCO, PAZU, PCHO, TRST) [Wdowski *et al.*, 1997]. They are located close enough to measure regionally coherent signals, such as large scale loading effects, and far enough not to be affected by local phenomena. The resulting common mode depicts no more than ± 2.5 mm of variations in the horizontal and ± 10 mm in the vertical without any trend over the period of interest (Fig. S1). Once time series are cleaned from all offsets and common-mode free, we detrend them with the ~ 1 -year trend estimated between early 2019 and the end of February 2020 (see Fig. S3).

For comparison with the previous SSE that occurred in 2014-2015 in the region, we use survey data from campaigns collected in the region almost every year over the last decade and until 2019 [from 2010, Métois *et al.*, 2014; Klein *et al.*, 2018b]. These observations are processed following the exact same methodology as the cGPS data. Resulting daily h-files at survey epochs (including adjusted parameters with their associated variance/covariance matrix) are combined with the continuous observations using PYACS [see more details in Klein *et al.*, 2022].

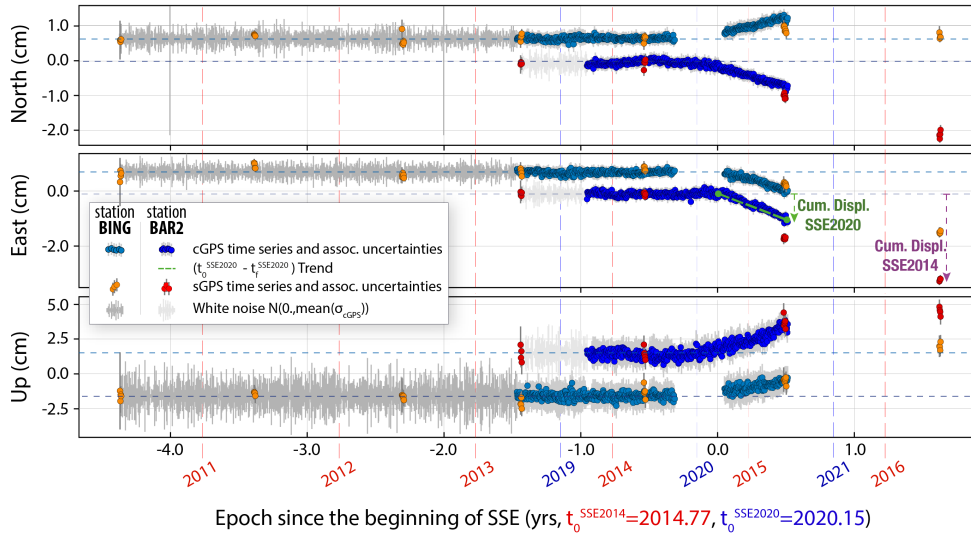


Figure 2. Comparison of sGPS sites BAR2 and BING time series (surveyed between 2013 and 2016: red, orange dots) with cGPS stations BAR2 and BING time series (upgraded in 2019: dark blue and light blue dots). Location of both stations are depicted on Fig. 1. All time series are aligned on the presumed date of beginning of each event (SSE2014: 2014.77, SSE2020: 2020.15). sGPS time series are detrended from the 2010-2014.5 trend, cGPS time series from the 2019-2020.0 trend. The BING time series are offset on the Y-axis for clarity. The trend estimated between the beginning of the SSE2020 and its end, used to compute the cumulative displacements is represented on North component of BAR2 cGPS time series. To highlight the coherence between sGPS and cGPS measurements before both SSEs, we extrapolated white noise with amplitude corresponding to each cGPS component mean uncertainties.

2.2 Data analysis

Many stations show an important deviation from their original trend on all three components, starting around March 2020 (ie. 2020.15, Fig. 1-B). The maximum deviation is observed at stations BAR2 and BING. Both stations are located near the coast, at the latitude of Copiapó (27.5°S). Other stations are located more to the south or more to the north and/or more inland. A striking feature is that while all stations move towards the west (trenchward), they diverge in terms of latitudinal displacement: northern stations move northward and southern stations southward. All stations also move upward, the maximum uplift being observed at BAR2, slightly south of Copiapó. Such a displacement pattern is already a clear indication of a deep source for this transient.

Continuous time series of 2020 compare very well to those from yearly surveys around 2014-2015. BAR2 and BING were survey sites, surveyed every year between 2010 (BING) or 2012 (BAR2) and 2016, before they were upgraded into continuous stations. BAR2 is exactly the same marker, BING is only several hundreds of meters away. At both locations, we split the complete (2010-2020) time series into two distinct periods: 2010-2017 (sGPS) on one side, 2017-2020 (cGPS) on the other side. We then aligned both periods on the presumed date of beginning of each event. Because we did not detect any other indicators, such as microseismicity or tremor, both these dates were estimated qualitatively. For the 2014 event (hereafter SSE2014), we estimated a beginning date of 2014.77, based on the COPO time series, the only cGPS station operational at the time (see Fig. S2). For the 2020 event (hereafter SSE2020), we estimated a beginning date of 2020.15. Both transients exhibit very similar patterns: uplift associated with trenchward motion and latitudinal divergence (Fig. 2). The amplitudes of the displacement reached after 6 months are also similar on all three com-

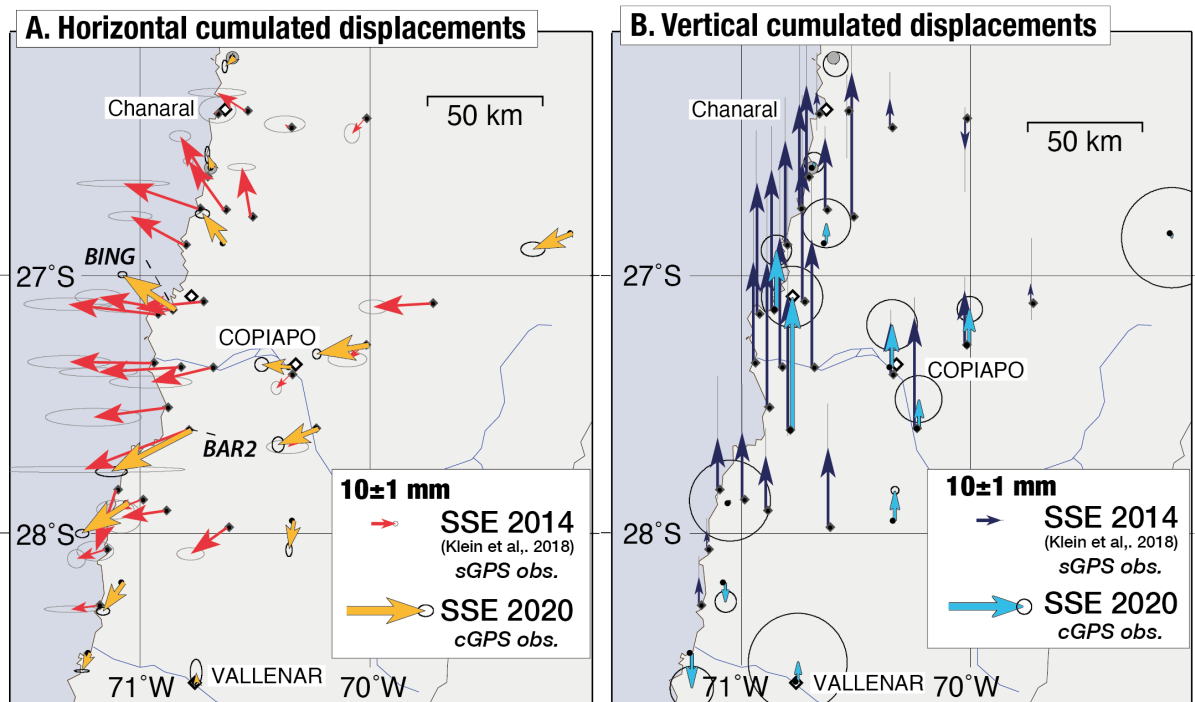


Figure 3. Comparison of cumulative displacements generated by SSE2014 over 18 months, and SSE2020 A) in horizontal (SSE2014=red, SSE2020=yellow); B) in vertical (SSE2014=dark blue, SSE2020=light blue). Beware that the scale of SSE2020 vectors is 3 times larger than the scale of SSE2014 vectors.

ponents. More pairs of sGPS sites-cGPS station are compared in the supporting material, showing the exact same pattern (Fig. S5).

The 2014 event reached a total displacement over three times larger than the 2020 event, but after a three-times longer duration (Fig. 3). Apart from this scale factor, the spatial pattern of both horizontal and vertical cumulative displacements compare very well, except within a narrow area north of Caldera. There, the 2020 event does not seem to have affected sites around the city of Chañaral (26.5°S), while the 2014 event did. Station BAR2 recorded the largest displacements, reaching 11 ± 2 mm in the horizontal and 17 ± 4 mm in the vertical component. Several other stations recorded smaller displacements around 5 ± 1 mm in the horizontal and 5 ± 3 mm in the vertical. The overall surface deformation is therefore modest, but still largely above - between 5 and 10 times - the typical noise of continuous observations (± 1 to 3 mm depending on the components).

3 Localisation of the source

The direct analysis of the cumulative surface displacements already reveals the main characteristics of the SSE2020 source: similar to SSE2014 with comparable amplitude, localisation and deep origin. In this section we perform a static inversion to quantify the exact location and amount of slip that was released over these 6 months.

3.1 Modeling strategy: Bayesian inversion

We use a Bayesian approach similar to the one used to study the SSE2014 [Klein *et al.*, 2018a]. We use the same fault geometry based on the finite element mesh designed in Klein

et al. [2016] between 28° S and 26° S down to 70 km depth, but with a higher resolution coming from patches 4 times smaller. The forward problem is defined as $\mathbf{d} = \mathbf{G}\mathbf{m}$ with \mathbf{d} , the vector containing GPS displacements and \mathbf{m} the slip model parameters. We assume a pure along-dip thrust faulting and Green's functions \mathbf{G} are calculated for each node of the fault plane, assuming a layered Earth model from [Husen *et al.*, 1999]. We explore the model-parameter space using a parallel Monte Carlo approach with AITar [Minson *et al.*, 2013; Duputel *et al.*, 2015; Jolivet *et al.*, 2015], to derive the posterior Probability Density Function (PDF) of the model \mathbf{m} given available observations \mathbf{d}_{obs} :

$$p(\mathbf{m}|\mathbf{d}_{\text{obs}}) \propto p(\mathbf{m}) \exp\left(-\frac{1}{2}(\mathbf{d}_{\text{obs}} - \mathbf{G}\mathbf{m})^T \mathbf{C}_x^{-1} (\mathbf{d}_{\text{obs}} - \mathbf{G}\mathbf{m})\right) \quad (1)$$

\mathbf{C}_x is defined as $\mathbf{C}_d + \mathbf{C}_p$ with \mathbf{C}_d describing observational uncertainties and \mathbf{C}_p representing forward model uncertainty. The novelty here compared to our previous work on SSE2014 is the introduction of the \mathbf{C}_p matrix. In particular, we account for the uncertainty resulting from inaccuracies in the Earth model used to compute our forward predictions. To derive this \mathbf{C}_p matrix, we rely on the formalism of [Duputel *et al.*, 2014] considering uncertainty on elastic properties similar to [Caballero *et al.*, 2021; Twardzik *et al.*, in press]. For the most part, this addition does not change the result of the inversion, but yields a refined determination of the posterior uncertainties. $p(\mathbf{m})$ is the prior PDF, defined as uniform with slip bounded between -1 cm and 50 cm (small back slip is allowed to ensure correct sampling near zero).

3.2 Slip distribution

The spatial extent of the SSE2014 was captured by survey GPS, while none of the cGPS stations captured the whole event. Therefore, at the time, we had excluded the less well determined vertical displacements from the inversion. Here, since we use cGPS, more reliable time series, we use both horizontal and vertical displacements to constrain the source slip model. The resulting posterior mean slip distribution shows significant slip over an area of about 25x25 km², located around 27.5°S, on the subduction interface between 40 and 60 km depth (Fig. 4-A). The maximum slip reaches a peak around 25 cm. Uncertainties associated with the slip distribution are not negligible (Fig. 4-B). This is mainly due to the high number of parameters compared to the relatively limited number of observations (Fig. S6). In addition, the inversion suggests slip stretched along the model deep boundary and apart from the main patch.

This deep slip in the posterior mean model is due to the large posterior uncertainty in the same area of the fault (Fig. 4-B). Such large posterior uncertainties at depth are caused by the lack of sensitivity of GPS observations to deep slip. When imposing slip positivity, the large uncertainty naturally leads to large posterior mean as illustrated with the marginal PDF for deep slip shown in Figure 4-C. Despite very large uncertainties in this area of the fault, notice that the maximum of the PDF remain close to 0 slip (See Fig. 4-C and D).

The fit to the data appears to be very good, with horizontal residuals of no more than 2 mm (Fig. 4-B). Vertical residuals are slightly larger, especially at station UDAT, the closest from Copiapó city, which is over-estimated by most models. The very small gradient between this station and those further east is a peculiar aspect of the data which is difficult to model. In any case, hundreds of models from the space of possible solutions show the persistence of the main deep patch of slip (cf. supporting information). We estimate a slip potency of $2.24 \pm 0.2 \cdot 10^8$ m.m² on this deep slip patch, corresponding to a moment of $1.31 \pm 0.1 \cdot 10^{19}$ N.m (Mw 6.7, see Fig. 4-A), considering a shear modulus of $5.87 \cdot 10^{10}$ Pa [Husen *et al.*, 1999].

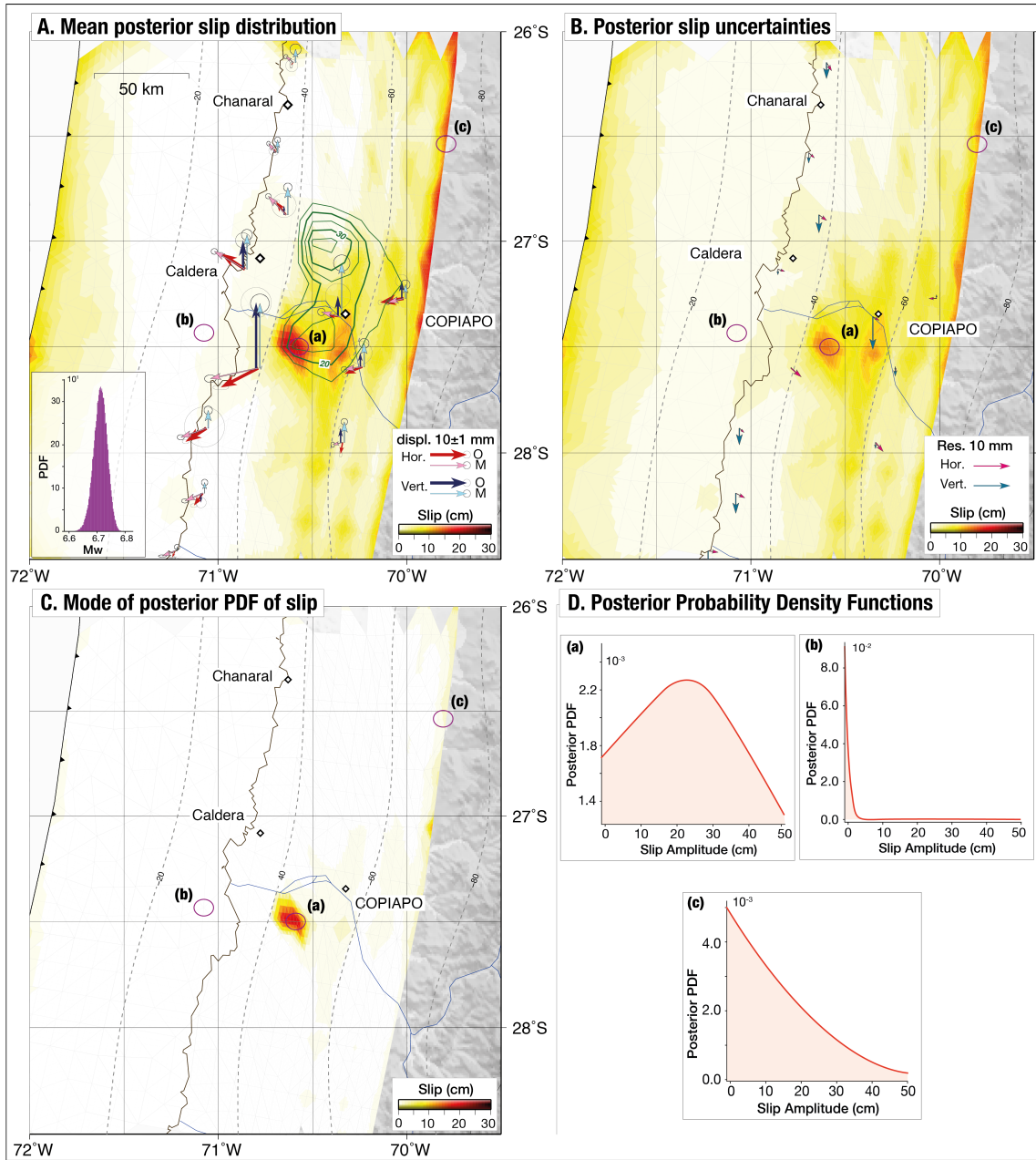


Figure 4. Slip model of the SSE2020. A. Mean posterior slip distribution in cm (represented by the white-to-red color scale). Observations are represented by the red (horizontal) and dark blue (vertical) arrows, compared to the model predictions in pink (horizontal) and light blue (vertical). The slip distribution of SSE2014 is represented by +5 cm green contours [Klein *et al.*, 2018a]. Inset shows the probability density function (PDF) of Mw of the deep patch of slip. B. 1σ posterior slip uncertainties represented with the same color scale as the slip distribution. Residuals (Obs.-Mod.) are represented by the red (horizontal) and blue (vertical) arrows. C. Mode of the posterior PDF of slip represented with the same color scale. D. Posterior Probability Density Functions of slip at 3 different patches (a) on the main slip region, (b) at shallow depth and (c) at deep depth, represented on each the 3 maps.

4 Discussions

4.1 Repetition of the 2014 Slow slip Event ?

The SSE2020 overlaps well the southern part of the SSE2014 (Fig. 4-A). In contrast, the northern area of the SS2014 seems unaffected by the 2020 event after the initial 6 months. This characteristic was already clear from the data, with very little displacements detected North of 26.9°S in 2020 (Fig. 1-B). We estimate a slip potency of the southern part of the SSE2014 (the one that corresponds to the SSE2020) of $8.83 \cdot 10^8 \text{ m.m}^2$, which is ~ 4 times larger than the slip potency of the SSE2020. This factor matches well the factor observed on displacements (see section 2.2). Because only sGPS data were available in 2014, we were unable to study the temporal evolution of the SSE2014. The single station that recorded the beginning of the event (COPO, Fig. S2), located roughly on top of the source center, does not allow to discriminate whether slip propagated in one direction or the other. However, it seems plausible that the 2014 SSE began in the South and that the slip produced by the 2020 event up to now replicates the first 6 months of 2014.

4.2 Interplay with the seismic/aseismic 2020 Atacama sequence

In the present study, we focused on the first 6 months of the returning slow slip event because of the occurrence of the seismic/aseismic sequence in September 2020 [Klein *et al.*, 2021]. This sequence started with a Mw6.9 on the megathrust zone on September, 1st, and was followed by a Mw6.4 aftershock 17 hours later (see Fig.1A). The study of micro seismicity migration and rapid afterslip between both events suggested that the aftershock was triggered by the upward propagation of aseismic slip. The whole sequence occurred offshore, south of the SSE2020 area (Fig. 1), but there was a clear interference between the two events. Several questions arise now regarding the interplay between the onset of this 2020 deep SSE (in March) and the sequence of September 1st, as well as regarding what happens next. Did the deep SSE play any role in the occurrence of the sequence ? Such complex interplay was observed in Mexico, where a SSE triggered the 7.3 Papanoa earthquake [Radiguet *et al.*, 2016]. Static inversion of the cumulative deformation may fail to uncover propagation to shallower depth. In turn, did the sequence perturb the deep SSE ? Did the sequence end the slow slip ? Did the slow slip continue regardless ? The deep patch of postseismic slip detected by kinematic inversions of the first month following the September sequence may support this last hypothesis [Klein *et al.*, 2021]. The similarity between the SSE2014 and the SSE2020 slip distributions also prompts us to make the assumption that the SSE2020 continued to propagate northward. Longer time series should reveal if the SSE2020 aborted after September or continued. They will also allow to analyze the spatio-temporal slip evolution through kinematic inversions.

4.3 Seismic hazard in the Atacama region

The SSE2020 occurred in the transition zone, downdip the highly coupled Atacama segment. The north extension of the SSE2014 also reached the transition zone downdip the Chanaral segment [Métois *et al.*, 2012; Métois *et al.*, 2016; Klein *et al.*, 2018b]. If the signal observed at COPO in 2009 is indeed the previous SSE [Klein *et al.*, 2018a], these coupling maps, derived from velocities estimated between 2010 and 2014, correspond to the inter-SSE period. Incidentally, it is remarkable that these recurrent SSEs occur within or near the downdip edge of the rupture zone of historical major earthquakes of the region: the 1819 Mw 8.5 and the 1922 Mw 8.6 [Willis, 1929; Kanamori *et al.*, 2019]. Even if precise slip distributions cannot be known, such events are large enough to rupture the entire seismogenic part of the interface. Located at the downdip end of plate contact, between 40 and 60 km deep, recurrent SSEs may regularly tickle the bottom of the locked zone that last ruptured exactly 100 years ago, and another 100 years ago before that. Even if Beeler *et al.* [2014] showed that large earthquake occurrence is not significantly enhanced by episodic deep slip events, the triggering of major subduction earthquakes due to stress load by deep SSE is

possible [Obara and Kato, 2016; Radiguet *et al.*, 2012]. Could one of these Copiapó SSEs have any play in the next major Atacama earthquake ?

4.4 The Role of the Copiapó Ridge

So far, the Atacama area ($\sim 27.5^\circ\text{S}$) is the only region of Chile where SSEs and non-volcanic tremors have been found. This is possibly due to the fact that the seismological and geodetic networks in Chile may not be dense enough to easily detect those events elsewhere [Barrientos and CSN Team, 2018; Báez *et al.*, 2018]. Nevertheless, the Atacama area is also a rheologically peculiar place because of the subduction at that latitude of the Copiapó Ridge. The presence of this subducted ridge seems to line up with these slow slip signatures and favor their occurrence. [Segovia *et al.*, 2018]. Its impact and the rheological changes it yields, such as an increase in the amount of fluids, changes in temperature, etc., should be studied and compared with other areas around the world, where SSEs are also observed periodically.

4.5 SSEs elsewhere in Chile

Although none were detected so far, SSEs are probably occurring in other regions of Chile. Seismic evidence, such as repeating earthquakes, seismic swarms and NVTs, were indeed detected in several regions along the Chilean subduction [Holtkamp *et al.*, 2011; Ide, 2012; Poli *et al.*, 2017; Sáez *et al.*, 2019; Valenzuela-Malebrán *et al.*, 2021]. Some of these events were suggested to be driven by the subduction of local features, for ex. seamount in Vichuquén, the Juan Fernandez Ridge and fracture zones in the oceanic Nazca plate. Incidentally, seismic swarms generally occur in areas of intermediate coupling, at the transition between low- and high-coupled segments [Métois *et al.*, 2016]. One of the main limitations to detect more SSEs is probably the density of the geodetic network, compared to those in Cascadia, Japan and New Zealand. The tectonic context in Atacama, in the interseismic phase about a century after the latest major earthquake, was favorable to detect the SSE2014 by survey GPS. In contrast, regions like Navidad (34.8°S) or Los Vilos (32°S), where swarms regularly occur, are strongly affected by the postseismic deformations following the 2010 Maule and 2015 Illapel earthquakes [Klein *et al.*, 2016; Boulze *et al.*, 2022]. In such a context, the survey GPS can not compensate for the low density of continuous stations.

4.6 Comparing with SSEs worldwide

This study confirms that the Chilean subduction zone is not so different from other subduction zones in terms of SSE occurrence. Although we only looked at the first 6 months, we hypothesize that the complete duration of the SSE2020 is similar to that of the SSE2014, therefore that both events have similar magnitudes. Considering the main features extracted from the SSE2014, the Copiapó SSEs align with the $\log M_o \sim \log T$ trend suggested for slow slip events [Ide *et al.*, 2007]. They are significantly longer than the Mexican events but similar in magnitude. SW Japan SSEs are comparable in duration but with significantly smaller magnitude [Gao *et al.*, 2012; Rousset, 2019]. The Copiapó SSEs appear very similar, in all characteristics, to the Manawatu and Kapiti SSEs in New Zealand [Obara, 2011; Wallace, 2020].

5 Conclusion

For a long time, very few SSEs were observed along the Chilean subduction zone, raising the debate on whether they did not take place there or if the observation networks were unable to detect them. Rather unusually, the first SSE2014 in the Atacama region was detected and quantified thanks to yearly repeated surveys in the area since 2010. Based on recent denser cGPS measurements, we now prove that this deep event has a periodicity of

5 years. We can therefore conclude that the Chilean subduction zone is in fact not so different from others where this type of event occurs, such as New Zealand [Wallace and Beavan, 2010], and in some ways Mexico and SW Japan [Hirose and Obara, 2005; Gao et al., 2012; Roussel, 2019]. However, we still have to confirm whether this SSE is characteristic, therefore identical, every 5 years or not.

Acknowledgments

This work was performed with financial support of the Institut National des Sciences de l'Univers (INSU-CNRS) Tellus program, the Agence Nationale de la Recherche (project ANR-19-CE31-0003) and the European Research Council (ERC) under the European Union's Horizon 2020 research and innovation program (grant agreement n°: 805256). SR thanks ANID/FONDECYT; project no. 1200779. We are also thankful to the INSU-CNRS and the Réseau Sismologique & Géodésique Français (RESIF, as part of the "Investissements d'Avenir" program, ANR-11-EQPX-0040, and the French Ministry of Ecology, Sustainable Development and Energy) for providing the geodetic instruments for all campaigns. We would like to warmly thank all CSN staff, for their precious help for the fieldwork. We thank Mark Simons (CalTech) for providing the AITar code used in this study and Romain Jolivet and Jean-Mathieu Nocquet for fruitful discussions. Finally, we sincerely thank Roland Bürgmann, our second anonymous reviewer for their very constructive reviews as well as the editor who handled our manuscript, Ana Ferreira. All the figures have been made using Generic Mapping Tools GMT [Wessel et al., 2013]. Python tool-boxes used: PYACS+PYEQ (<https://github.com/JMNocquet/pyacs36>), CSI (<http://www.geologie.ens.fr/jolivet/csi>)
Data availability: All time series of continuous GPS data used in this study come from the *SOAM_GNSS_solENS* database [Klein et al., 2022]). Time series of stations COP2020 over the considered period, will be made available upon publication of this study via the same repository as the solution.

References

- Báez, J., F. Leyton, C. Troncoso, F. del Campo, M. Bevis, C. Vigny, M. Moreno, M. Simons, E. Kendrick, H. Parra, et al. (2018), The Chilean GNSS network: Current status and progress toward early warning applications, *Seismological Research Letters*.
- Barrientos, S., and CSN Team (2018), The seismic network of Chile, *Seismological Research Letters*, 89(2A), 467–474.
- Beeler, N. M., E. Roeloffs, and W. McCausland (2014), Re-estimated effects of deep episodic slip on the occurrence and probability of great earthquakes in cascadia, *Bulletin of the Seismological Society of America*, 104(1), 128–144.
- Beroza, G. C., and S. Ide (2011), Slow earthquakes and nonvolcanic tremor, *Annual review of Earth and planetary sciences*, 39, 271–296.
- Boudin, F., P. Bernard, G. Meneses, C. Vigny, M. Olcay, C. Tassara, J. Boy, E. Aissaoui, M. Métois, C. Satriano, et al. (2022), Slow slip events precursory to the 2014 Iquique Earthquake, revisited with long-base tilt and GPS records, *Geophysical Journal International*, 228(3), 2092–2121.
- Boulze, H., L. Fleitout, E. Klein, and C. Vigny (2022), Post-seismic motion after 3 Chilean megathrust earthquakes: a clue for a linear asthenospheric viscosity, *Geophysical Journal International*, 231(3), 1471–1478.
- Caballero, E., A. Chounet, Z. Duputel, J. Jara, C. Twardzik, and R. Jolivet (2021), Seismic and aseismic fault slip during the initiation phase of the 2017 Mw= 6.9 Valparaíso earthquake, *Geophysical research letters*, 48(6), e2020GL091,916.
- Duputel, Z., P. S. Agram, M. Simons, S. E. Minson, and J. L. Beck (2014), Accounting for prediction uncertainty when inferring subsurface fault slip, *Geophys. J. Int.*, 197(1), 464–482.
- Duputel, Z., J. Jiang, R. Jolivet, M. Simons, L. Rivera, J.-P. Ampuero, B. Riel, S. Owen, A. Moore, S. Samsonov, et al. (2015), The Iquique earthquake sequence of April 2014:

- Bayesian modeling accounting for prediction uncertainty, *Geophysical Research Letters*, 42(19), 7949–7957.
- Gao, H., D. A. Schmidt, and R. J. Weldon (2012), Scaling relationships of source parameters for slow slip events, *Bulletin of the Seismological Society of America*, 102(1), 352–360.
- Hayes, G. P., D. J. Wald, and R. L. Johnson (2012), Slab1. 0: A three-dimensional model of global subduction zone geometries, *Journal of Geophysical Research: Solid Earth* (1978–2012), 117(B1).
- Herring, T., M. Floyd, and M. Perry (2018), Gamit/globk for gnss, *GNSS Data Processing and Analysis with GAMIT/GLOBK and track Hotel Soluxe, Bishkek, Kyrgyzstan*, pp. 2–7.
- Hirose, H., and K. Obara (2005), Repeating short-and long-term slow slip events with deep tremor activity around the Bungo channel region, southwest Japan, *Earth, planets and space*, 57(10), 961–972.
- Holtkamp, S. G., M. E. Pritchard, and R. B. Lohman (2011), Earthquake swarms in South America, *Geophysical Journal International*, 187(1), 128–146, doi:10.1111/j.1365-246X.2011.05137.x.
- Husen, S., E. Kissling, E. Flueh, and G. Asch (1999), Accurate hypocentre determination in the seismogenic zone of the subducting Nazca Plate in northern Chile using a combined on-/offshore network, *Geophysical Journal International*, 138(3), 687–701.
- Ide, S. (2012), Variety and spatial heterogeneity of tectonic tremor worldwide, *Journal of Geophysical Research: Solid Earth*, 117(B3).
- Ide, S., G. C. Beroza, D. R. Shelly, and T. Uchide (2007), A scaling law for slow earthquakes, *Nature*, 447(7140), 76.
- Jolivet, R., M. Simons, P. Agram, Z. Duputel, and Z.-K. Shen (2015), Aseismic slip and seismogenic coupling along the central San Andreas Fault, *Geophysical Research Letters*, 42(2), 297–306.
- Kanamori, H., L. Rivera, L. Ye, T. Lay, S. Murotani, and K. Tsumura (2019), New constraints on the 1922 Atacama, Chile, earthquake from historical seismograms, *Geophysical Journal International*, 219(1), 645–661.
- Klein, E., L. Fleitout, C. Vigny, and J. Garaud (2016), Afterslip and viscoelastic relaxation model inferred from the large scale postseismic deformation following the 2010 Mw 8.8 Maule earthquake (Chile), *Geophysical Journal International*, 205(3), 1455–1472, doi: 10.1093/gji/ggw086.
- Klein, E., Z. Duputel, D. Zigone, C. Vigny, J.-P. Boy, C. Doubre, and G. Meneses (2018a), Deep transient slow slip detected by survey GPS in the region of Atacama, Chile, *Geophysical research letters*, 45(22), 12–263.
- Klein, E., M. Métois, G. Meneses, C. Vigny, and A. Delorme (2018b), Bridging the gap between North and Central Chile : insight from new GPS data on coupling complexities and the Andean sliver motion, *Geophysical Journal International*, 213(3), 1924 – 1933.
- Klein, E., B. Potin, F. Pasten-Araya, R. Tissandier, K. Azua, Z. Duputel, C. Herrera, L. Rivera, J.-M. Nocquet, J.-C. Baez, et al. (2021), Interplay of seismic and a-seismic deformation during the 2020 sequence of Atacama, Chile, *Earth and Planetary Science Letters*, 570, 117,081.
- Klein, E., C. Vigny, J.-M. Nocquet, and H. Boulze (2022), A 20 year-long GNSS solution across South-America with focus in Chile, *Bulletin de la Société géologique de France*, doi:10.1051/bsgf/2022005.
- Métois, M., C. Vigny, and A. Socquet (2012), Interseismic coupling, segmentation and mechanical behavior of the central Chile subduction zone, *Journal of Geophysical Research*, 662, 120–131.
- Métois, M., C. Vigny, A. Socquet, A. Delorme, S. Morvan, I. Ortega, and C.-M. Valderas-Bermejo (2014), GPS-derived interseismic coupling on the subduction and seismic hazards in the Atacama region, Chile, *Geophysical Journal International*, 196(2), 644–655, doi:10.1093/gji/ggt418.
- Métois, M., C. Vigny, and A. Socquet (2016), Interseismic coupling, megathrust earthquakes and seismic swarms along the Chilean subduction zone (38–18° S), *Pure and Applied*

- Geophysics*, 173(5), 1431–1449.
- Minson, S., M. Simons, and J. Beck (2013), Bayesian inversion for finite fault earthquake source models I- theory and algorithm, *Geophysical Journal International*, p. ggt180.
- Nocquet, J.-M., and D. Tran (), PYACS Geodetic analysis and modeling tools for Tectonics, <https://github.com/JMNocquet/pyacs36>.
- Obara, K. (2011), Characteristics and interactions between non-volcanic tremor and related slow earthquakes in the nankai subduction zone, southwest japan, *Journal of Geodynamics*, 52(3-4), 229–248.
- Obara, K., and A. Kato (2016), Connecting slow earthquakes to huge earthquakes, *Science*, 353(6296), 253–257.
- Pastén-Araya, F., B. Potin, K. Azua, M. Saez, F. Aden-Antoniów, S. Ruiz, L. Cabrera, J.-P. Ampuero, J.-M. Nocquet, L. Rivera, et al. (2022), Along-dip segmentation of the slip behavior and rheology of the Copiapó Ridge subducted in North-Central Chile, *Geophysical Research Letters*, 49(4), e2021GL095471.
- Peng, Z., and J. Gombert (2010), An integrated perspective of the continuum between earthquakes and slow-slip phenomena, *Nature Geoscience*, 3(9), 599.
- Poli, P., A. Maksymowicz, and S. Ruiz (2017), The mw 8.3 illapel earthquake (chile): Pre-seismic and postseismic activity associated with hydrated slab structures, *Geology*, 45(3), 247–250.
- Radiguet, M., F. Cotton, M. Vergnolle, M. Campillo, A. Walpersdorf, N. Cotte, and V. Kostoglodov (2012), Slow slip events and strain accumulation in the Guerrero gap, Mexico, *Journal of Geophysical Research: Solid Earth*, 117(B4).
- Radiguet, M., H. Perfettini, N. Cotte, A. Gualandi, B. Valette, V. Kostoglodov, T. Lhomme, A. Walpersdorf, E. C. Cano, and M. Campillo (2016), Triggering of the 2014 Mw 7.3 Papanoa earthquake by a slow slip event in Guerrero, Mexico, *Nature Geoscience*, 9(11), 829.
- Rogers, G., and H. Dragert (2003), Episodic tremor and slip on the Cascadia subduction zone: The chatter of silent slip, *Science*, 300(5627), 1942–1943.
- Rousset, B. (2019), Months-long subduction slow slip events avoid the stress shadows of seismic asperities, *Journal of Geophysical Research: Solid Earth*, 124(7), 7227–7230.
- Ruiz, S., M. Metois, A. Fuenzalida, J. Ruiz, F. Leyton, R. Grandin, C. Vigny, R. Madariaga, and J. Campos (2014), Intense foreshocks and a slow slip event preceded the 2014 Iquique Mw 8.1 earthquake, *Science*, 345(6201), 1165–1169.
- Ruiz, S., F. Aden-Antoniow, J. Baez, C. Otarola, B. Potin, F. Campo, P. Poli, C. Flores, C. Satriano, F. Leyton, et al. (2017), Nucleation phase and dynamic inversion of the Mw 6.9 Valparaíso 2017 earthquake in Central Chile, *Geophysical Research Letters*, 44(20).
- Sáez, M., S. Ruiz, S. Ide, and H. Sugioka (2019), Shallow nonvolcanic tremor activity and potential repeating earthquakes in the chile triple junction: seismic evidence of the subduction of the active nazca–antarctic spreading center, *Seismological Research Letters*, 90(5), 1740–1747.
- Schwartz, S. Y., and J. M. Rokosky (2007), Slow slip events and seismic tremor at circum-pacific subduction zones, *Reviews of Geophysics*, 45(3).
- Segovia, M., Y. Font, M. Régnier, P. Charvis, A. Galve, J.-M. Nocquet, P. Jarrín, Y. Hello, M. Ruiz, and A. Pazmiño (2018), Seismicity distribution near a subducting seamount in the Central Ecuadorian subduction zone, space-time relation to a slow-slip event, *Tectonics*, 37(7), 2106–2123.
- Socquet, A., J. P. Valdes, J. Jara, F. Cotton, A. Walpersdorf, N. Cotte, S. Specht, F. Ortega-Culaciati, D. Carrizo, and E. Norabuena (2017), An 8 month slow slip event triggers progressive nucleation of the 2014 Chile megathrust, *Geophysical Research Letters*, 44(9), 4046–4053.
- Twardzik, C., Z. Duputel, R. Jolivet, E. Klein, and P. Rebischung (in press), Bayesian inference on the initiation phase of the 2014 Iquique, Chile, earthquake, *Earth and Planetary Sciences Letters*.

- Valenzuela-Malebrán, C., S. Cesca, S. Ruiz, L. Passarelli, F. Leyton, S. Hainzl, B. Potin, and T. Dahm (2021), Seismicity clusters in central chile: investigating the role of repeating earthquakes and swarms in a subduction region, *Geophysical Journal International*, 224(3), 2028–2043.
- Wallace, L. M. (2020), Slow slip events in new zealand, *Annual Review of Earth and Planetary Sciences*, 48, 175–203.
- Wallace, L. M., and J. Beavan (2010), Diverse slow slip behavior at the Hikurangi subduction margin, New Zealand, *Journal of Geophysical Research: Solid Earth*, 115(B12).
- Wdowinski, S., Y. Bock, J. Zhang, P. Fang, and J. Genrich (1997), Southern california permanent gps geodetic array: Spatial filtering of daily positions for estimating coseismic and postseismic displacements induced by the 1992 landers earthquake, *Journal of Geophysical Research: Solid Earth*, 102(B8), 18,057–18,070.
- Wessel, P., W. H. F. Smith, R. Scharroo, J. Luis, and F. Wobbe (2013), Generic Mapping Tools: Improved version released, *Eos, Transactions American Geophysical Union*, 94(45), 409–410, doi:10.1002/2013EO450001.
- Willis, B. (1929), *Studies in Comparative Seismology: Earthquake Conditions in Chile*, 382, Carnegie Institution of Washington.